# The Zeeman Effect in the Rotational Spectrum of Carbonyl Chloro Fluoride

F. Scappini * and A. Guarnieri

Abteilung für Chemische Physik im Institut für Physikalische Chemie der Universität Kiel

(Z. Naturforsch. **31 a**, 369–373 [1976]; received February 27, 1976)

The rotational Zeeman effect of FClCO is reported. The Chlorine nuclear $g_I$-factor, the molecular $g$-factors, $g_{aa}$, $g_{bb}$, and $g_{cc}$, and the magnetic susceptibility anisotropies, $(2\chi_{aa}-\chi_{bb}-\chi_{cc})_{\text{mole}}$ and $(2\chi_{bb}-\chi_{cc}-\chi_{aa})_{\text{mole}}$, are obtained from the spectrum.
Some derivative molecular quantities are calculated.

## 1. Introduction

Not many investigations of the rotational Zeeman effect of molecules containing a Chlorine atom have been reported up to now [1–4].

This laboratory has started to study such molecules in order to contribute to fill the present gap of informations. After the HOCl [5] and the $CH_3OCl$ [6] we took into consideration the FClCO molecule, whose $r_0$-structure is known [7]. The choice of small molecules is primarely determined by the fact that on these molecules it is possible to perform semi-empirical calculations to be compared to the experimental findings.

## 2. Experimental

The FClCO gas was made available to us in lecture bottle by P.C.R. Inc., Florida, U.S.A. Small samples were taken from time to time, condensed at dry ice temperature, and used for the spectroscopic analysis.

The Zeeman spectrometer is a conventional 33 kHz Stark modulated microwave one combined with a high stability, sufficient homogeneity electromagnet up to 30 kGauss. Details concerning the spectrometer can be found in Reference [8].

The absorption cell, with an effective length of 2.10 m, was cooled to about $-60\,^{\circ}\text{C}$ and the pressure of the gas was around 5 m Torr.

The Zeeman pattern of the rotational spectrum exhibited by this molecule has a rather poor intensity and a considerable overlapping occurs among the Zeeman satellites from different nuclear quadrupole components. These two facts have severely limited both the choice of the transitions and the choice of the magnetic field strength. The errors in the frequency measurements are believed to be less than $\pm 20$ kHz.

* On leave from Laboratorio di Spettroscopia Molecolare, Bologna, Italy.
Reprint requests to Prof. Dr. A. Guarnieri, Institut für Physikalische Chemie der Universität Kiel, Olshausenstraße 40–60, *D-2300 Kiel.*

## 3. Theoretical Review

The theoretical treatment of the rotational Zeeman effect in diamagnetic molecules having a quadrupole nucleus has been done by different authors [9–11]. The short outline which is given here is mainly intended to describe the computational procedure followed.

The effective Hamiltonian for a diamagnetic molecule having a nuclear quadrupole coupling with an imposed magnetic field can be expressed as:

$$\mathcal{H}=\mathcal{H}_{\mathrm{R}}+\mathcal{H}_{\mathrm{Q}}+\mathcal{H}_{\mathrm{H}} \tag{1}$$

where $\mathcal{H}_{\mathrm{R}}$ is the Hamiltonian operator for the pure rotational energy, $\mathcal{H}_{\mathrm{Q}}$ for the nuclear quadrupole interaction, and $\mathcal{H}_{\mathrm{H}}$ for the Zeeman interaction. This last term has three contributions

$$\mathcal{H}_{\mathrm{H}}=\mathcal{H}_{\mathrm{H}}^{(g)}+\mathcal{H}_{\mathrm{H}}^{(\chi)}+\mathcal{H}_{\mathrm{H}}^{(I)} \tag{2}$$

where $\mathcal{H}_{\mathrm{H}}^{(g)}$ is the Hamiltonian for the Zeeman effect due to the molecular $g$-factors, $\mathcal{H}_{\mathrm{H}}^{(\chi)}$ for the Zeeman effect due to the magnetic susceptibility anisotropies, and $\mathcal{H}_{\mathrm{H}}^{(I)}$ for the Zeeman effect of the quadrupole nucleus with the nuclear $g_I$-factor.

In the strong field case, where the Zeeman energies are larger than the quadrupole coupling energies, it is convenient to use the uncoupled basis, $|J, \tau, I, M_J, M_I\rangle$, to set up the matrix of the Hamiltonian (1). In this basis $\mathcal{H}_{\mathrm{R}}$ is diagonal, $\mathcal{H}_{\mathrm{H}}$ is approximated to be diagonal, and $\mathcal{H}_{\mathrm{Q}}$ is approximated to be diagonal in $J$, $\tau$, $I$, while it contributes with diagonal and off-diagonal elements in $M_J$ and $M_I$. Furthermore $\mathcal{H}_{\mathrm{Q}}$ is diagonal in $M_F = M_J + M_I$, and hence a factorisation into submatrices with common values of $M_J + M_I$ is possible. The

matrix elements of $\mathcal{H}_R$ and $\mathcal{H}_Q$ in the uncoupled basis, $|J, \tau, I, M_J, M_I\rangle$, are to be found in References [5, 9–11]. The matrix elements of the field dependent part, $\mathcal{H}_H$, are given further in this paper. The matrix of the Hamiltonian (1) has to be diagonalized in order to find the eigenvalues $E(J, \tau, I, M_J, M_I)$.

In the weak field case, where the Zeeman energies are smaller than the quadrupole coupling energies, the off-diagonal elements in the uncoupled basis are large in comparison to the differences between the diagonal elements which they connect and therefore it is more convenient to choose the coupled basis, $|J, \tau, I, F, M_F\rangle$, for the matrix of the Hamiltonian (1). The diagonalisation will lead to the eigenvalues $E(J, \tau, I, F, M_F)$.

In the present case the calculations have been made using the Hamiltonian (1) in the uncoupled basis, $|J, \tau, I, M_J, M_I\rangle$. However, since we never reached the completely uncoupled situation, in listing the Zeeman splittings, see Table 3, we referred to the $F, M_F$ designation of the Zeeman sublevels. Only for the $J = 0_{00} \rightarrow 1_{11}$ transition at a magnetic field strength of 25583 Gauss, with $\Delta M = 0$, we have nearly approached the uncoupled limiting case.

The first order energy expression corresponding to the Hamiltonian (2), in the uncoupled basis, has the form:

$$\begin{aligned} E_H(J, \tau, I, M_J, M_I) &= \langle J, \tau, I, M_J, M_I | \mathcal{H}_H | J, \tau, I, M_J, M_I \rangle \\ &= -\mu_0 \frac{M_J H_Z}{J(J+1)} \sum_g g_{gg} \langle J_g^2 \rangle - \tfrac{1}{2} \chi H_Z^2 \\ &\quad - H_Z^2 \frac{2M_J^2 - J(J+1)}{(2J-1)(2J+3)J(J+1)} \\ &\quad \cdot \sum_g (\chi_{gg} - \chi) \langle J_g^2 \rangle - \mu_0 g_I M_I H_Z \end{aligned} \tag{3}$$

where $g$ sums over the principal inertia axes, $a$, $b$, and $c$. $H_Z$ is the applied magnetic field, $g_{gg}$ is a diagonal element of the molecular $g$-tensor, $\chi_{gg}$ is a diagonal element of the magnetic susceptibility tensor, $\chi = \frac{1}{3}(\chi_{aa} + \chi_{bb} + \chi_{cc})$ is the bulk magnetic susceptibility, $g_I$ is the $g$-factor of the quadrupole nucleus, $\mu_0$ is the Bohr magneton, and $\langle J_g^2 \rangle$ is the expectation value of the squared angular momentum operator in the $J, \tau$ state.

A complete description of the magnetic properties of a rotating molecule containing a quadrupole nucleus is given by six independent constants, $g_I$, $g_{aa}$, $g_{bb}$, $g_{cc}$, $2\chi_{aa} - \chi_{bb} - \chi_{cc}$, and $2\chi_{bb} - \chi_{cc} - \chi_{aa}$, which enter in the Hamiltonian (1) through the field dependent part, $\mathcal{H}_H$. In same cases they, or at least their preliminary values, can be directly obtained from the spectrum using the procedure outlined in Reference [5]. These constants are finally fitted to all the Zeeman frequency splittings by a combined least squares fitting procedure.

## 3. Results

### *a) Nuclear and Molecular g-Values, and Magnetic Susceptibility Anisotropies*

In Table 1 are listed the zero-magnetic-field transitions which were found to be most suitable to study the Zeeman effect in the $\Delta_M = 0$ and in the $\Delta_M = \pm 1$ case.

Table 1. List of the zero-magnetic-field transitions used for the Zeeman analysis. The frequencies, in MHz, have been corrected for the nuclear quadrupole splittings. For the h.f.s. satellite frequencies see Table 3. The transitions refer to the isotopic species with Chlorine-35, as also all the other quantities observed and calculated in this paper.

| Transition | Corrected frequency obs. | calc. |
|---|---|---|
| $0_{00} \rightarrow 1_{01}$ | 8935.62 | 8935.62 |
| $0_{00} \rightarrow 1_{11}$ | 15479.04 | 15479.04 |
| $1_{11} \rightarrow 2_{12}$ | 16233.00 | 16233.00 |
| $1_{01} \rightarrow 2_{02}$ | 17600.32 | 17600.34 |

From these transitions the $A$, $B$, and $C$ rotational constants and the nuclear quadrupole constants were redetermined, see Table 2, with sligth differences from Reference [7].

Table 2. Rotational constants and nuclear quadrupole constants obtained from the transitions of Table 1. The errors reflect the experimental uncertainties.

| | |
|---|---|
| $A$ | $= 11830.35 \pm 0.03$ MHz |
| $B$ | $= 5286.93 \pm 0.03$ MHz |
| $C$ | $= 3648.69 \pm 0.03$ MHz |
| $\chi_{aa}^{Cl}$ | $-73.04 \pm 0.02$ MHz |
| $\chi_{bb}^{Cl}$ | $44.71 \pm 0.02$ MHz |
| $\chi_{cc}^{Cl}$ | $28.33 \pm 0.03$ MHz |

A summary of the frequency shifts from the zero-magnetic-field transitions at parallel and perpendicular magnetic field is given in Table 3.

Following the method described above, the six magnetic constants were obtained, see Table 4. The

Table 3. Zeeman spectrum at parallel and perpendicular magnetic field. The frequencies of the zero-magnetic-field transitions are also given. The calculated frequencies are according to Hamiltonian (1). Frequencies are in MHz and magnetic field strengths in Gauss.

| $J_{K-K+}$ $J'_{K'-K'+}$ | $F \rightarrow F'$ | Field | $M_F \rightarrow M_F$ | $\nu_{obs}$ | $\Delta\nu_{obs}$ * | $\Delta\nu_{calc}$ * |
|---|---|---|---|---|---|---|
| | | (parallel) | | | | |
| $0_{00} \rightarrow 1_{01}$ | 3/2 → 1/2 | 0 | | 89.53.88 | | |
| | | 13783 | 1/2 → 1/2 | 8952.53 | −1.35 | −1.33 |
| | | | −1/2 → −1/2 | 8956.48 | 2.60 | 2.60 |
| | 3/2 → 3/2 | 0 | | 8921.01 | | |
| | | 13428 | −3/2 → −3/2 | 8918.15 | −2.86 | −2.85 |
| | | | 3/2 → 3/2 | 8922.97 | 1.96 | 1.95 |
| | 3/2 → 5/2 | 0 | | 8939.27 | | |
| | | 13428 | −3/2 → −3/2 | 8936.19 | −3.08 | −3.07 |
| | | | −1/2 → −1/2 | 8938.73 | −0.54 | −0.54 |
| | | | 1/2 → 1/2 | 8941.07 | 1.80 | 1.79 |
| | | | 3/2 → 3/2 | 8943.25 | 3.98 | 3.98 |
| $0_{00} \rightarrow 1_{11}$ | 3/2 → 1/2 | 0 | | 15467.86 | | |
| | | 13428 | 1/2 → 1/2 | 15464.94 | −2.92 | −2.93 |
| | | | −1/2 → −1/2 | 15468.65 | 0.79 | 0.79 |
| | 3/2 → 3/2 | 0 | | 15487.98 | | |
| | | 11394 | −3/2 → −3/2 | 15486.41 | −1.57 | −1.57 |
| | | | 3/3 → 3/2 | 15490.67 | 2.69 | 2.67 |
| | 3/2 → 5/2 | 0 | | 15476.81 | | |
| | | 13415 | −3/2 → −3/2 | 15472.45 | −4.36 | −4.34 |
| | | | −1/2 → −1/2 | 15474.77 | −2.04 | −2.03 |
| | | | 1/2 → 1/2 | 15477.04 | 0.23 | 0.22 |
| | | | 3/2 → 3/2 | 15479.62 | 2.81 | 2.82 |
| | | 25583 | −1/2 → −1/2 | 15473.51 | −3.30 | −3.26 |
| | | | 1/2 → 1/2 | 15476.50 | −0.31 | −0.28 |
| | | | 3/2 → 3/2 | 15480.95 | 4.14 | 4.16 |
| $1_{11} \rightarrow 2_{12}$ | 1/2 → 3/2 | 0 | | 16244.18 | | |
| | | 3200 | −1/2 → −1/2 | 16243.12 | −1.06 | −1.01 |
| | | | 1/2 → 1/2 | 16245.33 | 1.15 | 1.15 |
| $1_{01} \rightarrow 2_{02}$ | 1/2 → 3/2 | 0 | | 17582.07 | | |
| | | 1950 | −1/2 → −1/2 | 17581.42 | −0.65 | −0.65 |
| | | | 1/2 → 1/2 | 17582.70 | 0.63 | 0.62 |
| | | (perpendicular) | | | | |
| $0_{00} \rightarrow 1_{01}$ | 3/2 → 1/2 | 0 | | 8953.88 | | |
| | | 5930 | −1/2 → 1/2 | 8950.65 | −3.23 | −3.22 |
| | | | −3/2 → −1/2 | 8952.40 | −1.48 | −1.49 |
| | | | 3/2 → 1/2 | 8955.60 | 1.72 | 1.72 |
| | | | 1/2 → −1/2 | 8957.34 | 3.46 | 3.45 |
| | 3/2 → 3/2 | 0 | | 8921.01 | | |
| | | 13604 | −1/2 → 1/2 | 8935.43 | −3.84 | −3.85 |
| | | | 1/2 → 3/2 | 8937.65 | −1.62 | −1.63 |
| | | | −3/2 → −5/2 | 8938.93 | −0.34 | −0.34 |
| | | | 3/2 → 5/2 | 8939.62 | 0.35 | 0.34 |
| $0_{00} \rightarrow 1_{11}$ | 3/2 → 3/2 | 0 | | 15487.98 | | |
| | | 13578 | −1/2 → 1/2 | 15485.09 | −2.89 | −2.90 |
| | | | 1/2 → 3/2 | 15485.64 | 2.34 | 2.34 |
| | | | −1/2 → −3/2 | 15491.86 | 3.88 | 3.88 |
| | 3/2 → 5/2 | 13578 | −3/2 → −5/2 | 15476.29 | −0.52 | −0.52 |
| | | | 3/2 → 5/2 | 15477.34 | 0.53 | 0.52 |
| | | | −1/2 → −3/2 | 15478.05 | 1.24 | 1.25 |

* $\Delta\nu_{obs}$ and $\Delta\nu_{calc}$ are the differences between the frequencies of the split and the unsplit lines.

Table 4. Experimental Zeeman parameters: Chlorine nuclear $g_I$-factor, molecular $g$-factors, and magnetic susceptibility anisotropies. The quoted uncertainties are standard errors from the least squares fitting procedure. They do not account for errors introduced by the neglect of vibrations.

| | |
|---|---|
| $g_I = 0.5461 \pm 0.0010$ | $g_{bb} = -0.021 \pm 0.012$ |
| $g_{aa} = 0.056 \pm 0.011$ | $g_{cc} = -0.044 \pm 0.010$ |
| $(2\chi_{aa} - \chi_{bb} - \chi_{cc})_{\text{mole}} = (-1.63 \pm 1.29) \cdot 10^{-6}$ erg/G$^2$·mole | |
| $(2\chi_{bb} - \chi_{cc} - \chi_{aa})_{\text{mole}} = (3.01 \pm 0.63) \cdot 10^{-6}$ erg/G$^2$·mole | |

signs of the molecular $g$-factors, $g_{gg}$, could be unambigously determined since the sign of the Chlorine $g_I$-factor is known to be positive [12].

### *b) Second Moment Electronic Charge Anisotropies, Magnetic Susceptibilities and Molecular Quadrupole Moments*

The anisotropies in the second moments may be related to the known molecular structure and the experimental Zeeman constants as follows:

$$\begin{aligned}\langle b^2\rangle - \langle a^2\rangle &= \langle 0 | \sum_i (b_i - a_i) | 0\rangle \\ &= \sum_n Z_n (b_n^2 - a_n^2) + \frac{\hbar}{4\pi M}\left(\frac{g_{bb}}{B} - \frac{g_{aa}}{A}\right) \\ &= \frac{4 m c^2}{3 e^2 N}(2\chi_{bb} - \chi_{aa} - \chi_{cc})_{\text{mole}} \\ &\quad - (2\chi_{aa} - \chi_{bb} - \chi_{cc})_{\text{mole}}\end{aligned} \tag{4}$$

where $Z_n$ is the atomic number of the $n$-th nucleus, $a_n$ and $b_n$ are its coordinates in the principal inertial axis system, $a_i$ and $b_i$ are the coordinates of the $i$-th electron in the principal inertial axis system, $M$ is the proton mass, $e$ is the electron charge, $N$ is the Avogadro's number, and $\langle 0 | | 0\rangle$ indicates the expectation value in the ground electronic state. The subscript "mole" designates molar quantities. Similar expressions for $\langle c^2\rangle - \langle b^2\rangle$, and $\langle a^2\rangle - \langle c^2\rangle$ are obtained by cyclic permutations of $a$, $b$ and $c$.

The value of the nuclear second moments were calculated from Ref. [7] and the rotational constants of the present work. They are, in units of $10^{-16}$ cm$^2$:

$$\sum_n Z_n a_n^2 = 95.7 \pm 1.0\,, \quad \sum_n Z_n b_n^2 = 42.7 \pm 0.5\,,$$
$$\sum_n Z_n c_n^2 = 0.0\,.$$

Since the known molecular structure is a $r_0$-structure an uncertainty of 1% on the above quantities seemed to be reasonable. Using the empirical additivity rules [13] to compute the out-of-plane second moment of the charge distribution, $\langle c^2\rangle$, the values of $\langle a^2\rangle$ and $\langle b^2\rangle$ are obtained from the second moment electronic charge anisotropies.

The diagonal elements of the paramagnetic susceptibility tensor can be calculated according to:

$$\chi^{\text{p}}_{aa,\,\text{mole}} = -\frac{e^2 N}{4 m c^2}\left[\frac{\hbar\, g_{aa}}{4\pi A M} - \sum_n Z_n (b_n^2 + c_n^2)\right]. \tag{5}$$

The diagonal elements of the diamagnetic susceptibility tensor are given by:

$$\chi^{\text{d}}_{aa,\,\text{mole}} = -\frac{e^2 N}{4 m c^2}(\langle b^2\rangle + \langle c^2\rangle)\,. \tag{6}$$

The diagonal elements of the total susceptibility tensor are found by adding together the corresponding paramagnetic and diamagnetic terms. Finally the total (or bulk) susceptibility is calculated according to:

$$\chi_{\text{bulk}} = \tfrac{1}{3}(\chi_{aa} + \chi_{bb} + \chi_{cc})_{\text{mole}}\,. \tag{7}$$

No measurement of the bulk susceptibility was done due to the experimental difficulties connected with the chemistry of the compound.

The molecular quadrupole moments in the principal inertial axis system may be obtained from the expression:

$$Q_{aa} = \frac{\hbar\,|e|}{8\pi M}\left(\frac{2\,g_{aa}}{A} - \frac{g_{bb}}{B} - \frac{g_{cc}}{C}\right) - \frac{2 m c^2}{|e| N} \cdot (2\chi_{aa} - \chi_{bb} - \chi_{cc})_{\text{mole}}\,. \tag{8}$$

All the quantities calculated as discussed above are listed in Table 5.

Table 5. Calculated Zeeman parameters: second moment of electronic charge anisotropies, second moments of electronic charge distributions, magnetic susceptibilities, total susceptibility, and molecular quadrupole moments. The quoted uncertainties come from the standard errors propagation. A 10% error was assumed in $\langle c^2\rangle$.

| | |
|---|---|
| $\langle b^2\rangle - \langle a^2\rangle$ | $(-52.2 \pm 1.2) \cdot 10^{-16}$ cm$^2$ |
| $\langle c^2\rangle - \langle b^2\rangle$ | $(-47.1 \pm 1.6) \cdot 10^{-16}$ cm$^2$ |
| $\langle a^2\rangle - \langle c^2\rangle$ | $(99.3 \pm 2.2) \cdot 10^{-16}$ cm$^2$ |
| $\langle a^2\rangle$ | $(105.1 \pm 2.3) \cdot 10^{-16}$ cm$^2$ |
| $\langle b^2\rangle$ | $(52.9 \pm 1.7) \cdot 10^{-16}$ cm$^2$ |
| $\langle c^2\rangle$ | $(5.8 \pm 0.6) \cdot 10^{-16}$ cm$^2$ |
| $\chi^{\text{p}}_{aa,\,\text{mole}}$ | $(191.2 \pm 2.1) \cdot 10^{-6}$ erg/G$^2$·mole |
| $\chi^{\text{p}}_{bb,\,\text{mole}}$ | $(414.3 \pm 4.2) \cdot 10^{-6}$ erg/G$^2$·mole |
| $\chi^{\text{p}}_{cc,\,\text{mole}}$ | $(612.7 \pm 4.7) \cdot 10^{-6}$ erg/G$^2$·mole |
| $\chi^{\text{d}}_{aa,\,\text{mole}}$ | $(-249.1 \pm 7.6) \cdot 10^{-6}$ erg/G$^2$·mole |
| $\chi^{\text{d}}_{bb,\,\text{mole}}$ | $(-470.6 \pm 10.0) \cdot 10^{-6}$ erg/G$^2$·mole |
| $\chi^{\text{d}}_{cc,\,\text{mole}}$ | $(-670.5 \pm 12.1) \cdot 10^{-6}$ erg/G$^2$·mole |
| $\chi_{aa,\,\text{mole}}$ | $(-57.9 \pm 7.9) \cdot 10^{-6}$ erg/G$^2$·mole |
| $\chi_{bb,\,\text{mole}}$ | $(-56.3 \pm 10.8) \cdot 10^{-6}$ erg/G$^2$·mole |
| $\chi_{cc,\,\text{mole}}$ | $(-57.8 \pm 13.0) \cdot 10^{-6}$ erg/G$^2$·mole |
| $\chi_{\text{bulk}}$ | $(-57.3 \pm 6.7) \cdot 10^{-6}$ erg/G$^2$·mole |
| $Q_{aa}$ | $(-7.0 \pm 3.1) \cdot 10^{-26}$ esu·cm$^2$ |
| $Q_{bb}$ | $(-12.4 \pm 6.6) \cdot 10^{-26}$ esu·cm$^2$ |
| $Q_{cc}$ | $(19.4 \pm 7.3) \cdot 10^{-26}$ esu·cm$^2$ |

## 4. Conclusion and Discussion

The signs and the magnitude of the molecular quadrupole moments along the principal axes are determined by the distribution of charge in the molecule, as schematically illustrated, together with the molecular structure, in Figure 1. Due to the

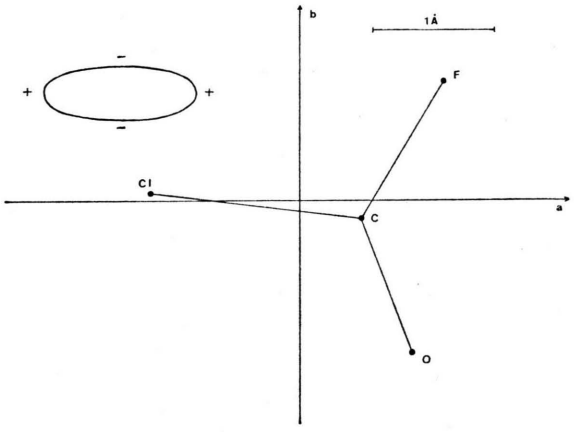


Fig. 1. Molecular structure of FClCO and charge distribution in the *a*, *b* plane.

errors on $Q_{aa}$ and $Q_{bb}$ not much can be said about the in-plane charge distribution. We may only discuss the two limiting possibilities: $Q_{aa} > Q_{bb}$ and $Q_{aa} < Q_{bb}$. The first one, besides it is more probable according to the error distribution law, is also supported by the results of an analysis of the principal elements of the nuclear quadrupole coupling tensor. Assuming the $z$-prinzipal axis of the nuclear quadrupole coupling tensor collinear with the C – Cl bond and the $x$-axis in the molecular plane, the diagonal (principal) elements are calculated[14] to be:

$$\chi_{xx}^{Cl} = 46.46\ \text{MHz}, \quad \chi_{yy}^{Cl} = 28.32\ \text{MHz},$$
$$\chi_{zz}^{Cl} = -74.78\ \text{MHz}.$$

The computation[14] based on the above quantities leads to a contribution of 11% from the structure containing the Chlorine, double bonded to the Carbon, in the $Cl^+$ form. Correspondingly the Oxigen becomes negative. Therefore, since the Chlorine is very close to the $a$-axis and the Oxigen is closer to the $b$-axis than to the $a$-axis, it is reasonable to assume a charge distribution less negative along the $a$-axis than along the $b$-axis, in accordance with the sequence $Q_{aa} > Q_{bb}$.

The value of $Q_{cc}$, out of plane moment, looks high. Its positive value indicates a charge attraction exerted by the electronegative atoms on the $\pi$ bond electrons. The same trend, i. e. $Q_{cc} > 0$, is present in $COF_2$[15] and CHOF[16].

The magnetic susceptibility anisotropies are very small, see Table 5. Consequently the spectrum is rather insensitive to the second order Zeeman effect, at the field strengths used for the measurements, and the relative errors on the corresponding quantities are considerable.

Semiempirical calculations, as mentioned in the Introduction, are postponed until a sufficient number of Chloro-containing molecules will be studied to allow a systematic discussion of their magnetic characteristics.

*Acknowledgements*

The authors want to thank Dr. M. Suzuki, Prof. H. Dreizler, and Prof. D. Sutter for helpful discussions, and Dr. E. Hamer for his contribution to the computing program. – The research funds and the research grant (F.S.) of the "Deutsche Forschungsgemeinschaft" and of the "Fonds der Chemie" are acknowledged. – Calculations have been made with the PDP 10 computer of the "Rechenzentrum der Universität Kiel".

[1] D. L. Vanderhart and W. H. Flygare, Mol. Phys. **18**, 77 [1970].
[2] J. McGurk, C. L. Norris, H. L. Tigelaar, and W. H. Flygare, J. Chem. Phys. **58**, 3118 [1973].
[3] J. J. Ewing, H. L. Tigelaar, and W. H. Flygare, J. Chem. Phys. **56**, 1957 [1972].
[4] C. L. Allen and W. H. Flygare, Chem. Phys. Lett. **15**, 461 [1972].
[5] M. Suzuki and A. Guarnieri, Z. Naturforsch. **30 a**, 497 [1975].
[6] M. Suzuki and A. Guarnieri, private communication.
[7] A. Guarnieri, A. M. Mirri, P. Favero, and L. Grifone, Ric. Sc. vol. 1, **3**, 358 [1961]. – A. M. Mirri, A. Guarnieri, P. Favero, and G. Zuliani, Nuovo Cim. **25**, 265 [1962].
[8] D. Sutter, Z. Naturforsch. **26 a**, 1644 [1971].
[9] W. Hüttner and W. H. Flygare, J. Chem. Phys. **47**, 4137 [1967].
[10] E. Hamer, Thesis, University of Kiel 1974, Chapter IV.
[11] D. Sutter and W. H. Flygare, Topics in Current Chemistry **63**, [1976] – in press.
[12] Y. Saito, Canadian J. Chem. **43**, 2530 [1965].
[13] T. D. Gierke, H. L. Tigelaar, and W. H. Flygare, J. Amer. Chem. Soc. **94**, 330 [1972].
[14] W. Gordy and R. L. Cook, Microwave Molecular Spectra, Interscience Publishers (1970), Chapters IX and XIV.
[15] R. P. Blikensderfer, J. H. S. Wang, and W. H. Flygare, J. Chem. Phys. **51**, 3196 [1969].
[16] S. L. Rock, J. K. Hancock, and W. H. Flygare, J. Chem. Phys. **54**, 3450 [1971].